Catal Lett (2008) 121:1–11
DOI 10.1007/s10562-007-9288-1

Fischer–Tropsch Synthesis: Characterization Rb Promoted Iron Catalyst

Amitava Sarkar · Gary Jacobs · Yaying Ji · Hussein H. Hamdeh · Burtron H. Davis

Received: 17 August 2007 / Accepted: 25 September 2007 / Published online: 1 November 2007

Abstract Rubidium promoted iron Fischer–Tropsch synthesis (FTS) catalysts were prepared with two Rb/Fe atomic ratios (1.44/100 and 5/100) using rubidium nitrate and rubidium carbonate as rubidium precursors. Results of catalytic activity and deactivation studies in a CSTR revealed that rubidium promoted catalysts result in a steady conversion with a lower deactivation rate than that of the corresponding unpromoted catalyst although the initial activity of the promoted catalyst was almost half that of the unpromoted catalyst. Rubidium promotion results in lower methane production, and higher CO_2, alkene and 1-alkene fraction in FTS products. Mössbauer spectroscopic measurements of CO activated and working catalyst samples indicated that the composition of the iron carbide phase formed after carbidization was χ-Fe_5C_2 for both promoted and unpromoted catalysts. However, in the case of the rubidium promoted catalyst, ε'-$Fe_{2.2}C$ became the predominant carbidic phase as FTS continued and the overall catalyst composition remained carbidic in nature. In contrast, the carbide content of the unpromoted catalyst was found to decline very quickly as a function of synthesis time. Results of XANES and EXAFS measurements suggested that rubidium was present in the oxidized state and that the compound most prevalent in the active catalyst samples closely resembled that of rubidium carbonate.

A. Sarkar · G. Jacobs · Y. Ji · B. H. Davis (✉)
Center for Applied Energy Research, University of Kentucky, 2540 Research Park Drive, Lexington, KY 40511, USA
e-mail: davis@caer.uky.edu

H. H. Hamdeh
Department of Physics, Wichita State University, Wichita, KS 67260, USA

Keywords Fischer–Tropsch synthesis · Iron catalyst · Rubidium · Active species · Mössbauer · XANES · EXAFS · Alkali promoters

1 Introduction

Iron-based Fischer–Tropsch Synthesis (FTS) catalysts are preferred for utilizing synthesis gas derived from coal or biomass because of their excellent activity in water gas shift (WGS) reaction which allows using a synthesis gas with a low H_2/CO ratio (typically 0.7) directly without an upstream water gas shift unit. The use of iron-based catalysts is also attractive in view of their lower cost, lower methane selectivity, high olefin-selectivity, lower sensitivity towards poisons and flexible product slate. The impact of Group I alkali promoters (i.e., Li, Na, K, Rb, and Cs) on the activity, kinetic parameters and selectivity of iron based catalysts for FTS and WGS reaction have been studied [1–6]. The relative impact of the alkali metals depends on the conversion level and the basicity of the metal. It is believed that strong basicity of Group I metals have significant effects on both FTS activity and product selectivity [1]. Potassium has been used extensively as the promoter which offers the greatest benefit at a lower price than other Group I alkali metals. It was claimed that potassium enhances the adsorption of CO and decreases the adsorption of H_2; therefore, in this view, potassium decreases secondary hydrogenation of alkenes. The results were explained by the fact that potassium donates electrons to iron and facilitates chemisorption of CO which tends to accept electrons from iron. Hydrogen at higher surface coverage, however, is prone to act as electron donor to iron. Thus the presence of potassium is considered to weaken the strength of the Fe–H bond [1, 7]. Potassium

salts are widely used as the most effective promoter in iron-based catalysts; however, the readiness to form an alkali compound with common catalyst supports, or structural promoters such as alumina or silica, complicates the situation.

The effects of potassium on the FTS and WGS activities and product selectivities have been investigated over a variety of iron-based catalysts [3, 5, 7–11]. The significant promoting effects of potassium can be summarized as follows: (1) favors the dissociative chemisorption of CO, strengthens the Fe–C bond and weakens the Fe–H bond; (2) enhances the selectivity of long-chain products and olefin selectivity, lowers methane selectivity; (3) increases WGS activity; (4) influences FTS activity. Although, potassium enhances the FTS activity and heavy product fraction, high potassium loading may cover too large of a fraction of the surface of the iron catalyst, resulting in a limited promotion effect or even a decrease in CO conversion [6]. Li et al. [3–5] concluded that potassium promotes the formation of an increased number of active sites during reduction and carbidization of iron oxides (i.e., by facilitating the rapid formation of nucleation sites resulting in the formation of smaller iron carbide crystallites). It was also suggested that potassium apparently present as carbonate form plays a role as a structural promoter; however, no experimental results were provided to support this claim [4].

In order to determine the chemical compound that most closely represents the state of the alkali promoter in the working catalyst under the FTS environment, rubidium was selected as the promoter in the present study. Rubidium, though less effective as a promoter, has an electronic transition that can be readily studied by EXAFS and XANES synchrotron techniques [12]. In addition, the oxides of rubidium has been reported to be "superbases", possessing base strengths with a Hammett basicity function, H_-, exceeding +26 [13]. Hence, it is believed that that supported oxide of rubidium also exhibit strong basicity [14]. In our previous investigation [2] on rubidium promoted iron catalyst with Rb/Fe atomic ratio of 1.44/100 [catalyst composition: 100Fe/4.6Si/1.44Rb], rubidium was found to (1) decrease the overall CO conversion; (2) increase the deactivation rate; (3) decrease the WGS rate as a function of inverse of space velocity (i.e., 1/SV); (4) improve the product selectivity by decreasing the C_2–C_4 selectivity and increasing the higher molecular weight fraction (C_{5+}); (5) decrease the methane selectivity; and (6) increase the C_2 alkene/alkane selectivity. It was also concluded that apart from WGS activity, the basicity of the Group I promoter (Li, Cs and Rb) defines the relative catalytic activity. However, due to lack of detailed knowledge on the nature of the chemical compound that represent the alkali promoter in the working catalyst, a direct comparison of alkali metal promoter based on the position in the periodic table is not reasonable. Although the effects of rubidium promotion on the FTS performances of iron-based catalysts have been reported in the above study, no results have been reported about the chemical state of alkali metal promoter, phase composition and characterization of the working catalyst.

The present research focuses on a systematic characterization of rubidium promoted ultrafine iron catalyst during activation and FTS. Particular attention is given to the effect of rubidium on extent of catalyst carbidization and bulk phase composition, and also to identify the chemical nature of rubidium compound that represents chemical state of the promoter in rubidium promoted working FTS catalyst. Rubidium carbonate (decomposition temperature = 740 °C) and rubidium nitrate (decomposition temperature = 219 °C) were used as rubidium precursors. If rubidium exists as carbonate form in the working rubidium promoted FTS catalyst, then in the case of rubidium promoted catalyst prepared from rubidium nitrate precursor, the rubidium nitrate should also transform into rubidium carbonate form when FTS is effected at a temperature that is higher than the decomposition temperature of rubidium nitrate. Bulk phase compositions of rubidium promoted and unpromoted catalysts after activation and during FTS were determined using Mössbauer spectroscopy. XANES measurements were used to identify the chemical nature of the rubidium species present during FTS for rubidium promoted catalysts prepared from carbonate and nitrate precursors. Results from these measurements are important to determine any potential transformation of rubidium nitrate to rubidium carbonate form in the working FTS catalyst. Also the chemical state of iron present in the catalyst during FTS was compared using a combination of XANES, EXAFS, and Mössbauer spectroscopy.

2 Experimental

2.1 Catalyst Preparation

A commercial ultrafine iron oxide catalyst (NANOCAT® Superfine Iron Oxide, Mach I, Inc.; 3–5 nm particle size, surface area = 250 m^2/g, and bulk density = 0.05 g/cm^3) was used to prepare the rubidium promoted catalyst using the rubidium nitrate precursor. A catalyst with Rb to Fe atomic ratio of 5.0/100 was prepared using rubidium nitrate (99.99%, 204269, Sigma–Aldrich, Inc.) as the precursor and is designated as 5RbN. A well-studied iron catalyst was split into two separate batches and promoted with rubidium using rubidium carbonate (99.8%, 251437, Sigma–Aldrich, Inc.) precursor at two Rb to Fe atomic ratio levels: 1.44/100 and 5.0/100. These catalysts are designated as catalysts 1.44RbC and 5RbC, respectively.

The two loadings were used, because it was difficult to assess whether the Rb signal would be observed by X-ray absorption spectroscopies in the catalyst with the lower loading. The precipitated iron catalyst used to prepare 1.44RbC and 5RbC was prepared with tetraethyl orthosilicate, iron nitrate, potassium carbonate and copper nitrate. Ferric nitrate solution was first prepared by dissolving $Fe(NO_3)_3$ in deionized water, and the amount of orthosilicate needed to make Si:Fe atomic ratio of 4.6:100 was added. The mixture was stirred vigorously until the tetraethyl orthosilicate was hydrolyzed. Tetraethyl orthosilicate and iron nitrate mixture was then added to a CSTR precipitator vessel together with a separate stream of ammonium hydroxide. By maintaining the slurry pH at 9 and an average residence time of 6 min, a base catalyst material with an iron to silicon molar ratio of 100:4.6 was obtained. The slurry was then filtered with a vacuum drum filter and washed twice with deionized water. The final filtration cake was dried in an oven with flowing air at 110 °C for 24 h. The catalyst was crushed and calcined at 350 °C under an air flow for 4 h. Rubidium was added to obtain a Rb/Fe atomic ratio of either 1.44/100 or 5.00/100 using a slurry phase impregnation technique. In the slurry phase impregnation method, the ratio of the volume of aqueous solution of rubidium precursor used to the weight of the support was 1:1, such that approximately 2.5 times the pore volume of solution was totally used to achieve the final target rubidium loading of the catalyst. Multiple impregnation steps were used and between each step the catalyst was dried under vacuum in a rotary evaporator at 60 °C and the temperature was slowly raised to 110 °C and maintained for 8 h. After the final impregnation/drying step, the catalyst was calcined at 350 °C overnight.

2.2 Reaction Testing

The FTS experiments were conducted in a 1 L CSTR equipped with a magnetically driven stirrer with turbine impeller, a gas-inlet line, and a vapor outlet line with a SS fritted filter (2 micron) placed external to the reactor. A tube fitted with a SS fritted filter (0.5 micron opening) extends below the liquid level of the reactor for withdrawing reactor wax (rewax, solid at room temperature) maintaining a constant liquid level in the reactor. Another SS dip-tube (1/8 in. OD), extending to the bottom of the reactor, was used to withdraw catalyst/wax slurry from the reactor at different synthesis times. Separate mass flow controllers were used to control the flow of hydrogen and carbon monoxide at the desired rate. The gases were premixed in a mixing vessel before entering the reactor. Carbon monoxide was passed through a vessel containing lead oxide-alumina to remove any traces of iron carbonyl. The mixed gases entered the CSTR below the stirrer operated at 750 rpm. The reactor temperature was maintained constant (± 1 °C) by a temperature controller. Polywax 3000 (PW3000, polyethylene fraction with average molecular weight of 3,000) purchased from Baker Petrolite, Inc. was used as the start-up solvent.

Three catalysts (unpromoted ultrafine iron oxide catalyst, 5RbC and 5RbN) were tested for activity and to make a comparison of the deactivation rate. The catalyst (ca. 55 g) was added to melted (150 °C) Polywax 3000 (310 g) in the CSTR to produce a slurry that contained about 15 wt% solids. The reactor temperature was then raised to 270 °C at a rate of 1 °C/min. The catalyst was activated using CO at a space velocity of 3.0 sl/h/g Fe at 270 °C and 175 psi g for 24 h. At the end of the activation period, a sample of activated catalyst was withdrawn via the slurry withdrawal dip-tube of the CSTR. FTS was then started by adding synthesis gas mixture to the reactor at a space velocity of 3.0 sl/h/g Fe and a H_2/CO ratio of 0.7. The conversions of CO and H_2 were obtained by GC analysis (HP Quad Series Micro-GC equipped with thermal conductivity detectors) of the product gas mixture. The reaction products were collected in three traps maintained at different temperatures—a hot trap (200 °C), a warm trap (100 °C) and a cold trap (0 °C). The products were separated into different fractions (rewax, wax, oil and aqueous) for quantification by GC analysis. However, the oil and the wax (liquid at room temperature) fractions were mixed prior to GC analysis. Catalyst/rewax slurry was withdrawn at different reaction times via the dip-tube after sufficient purging. In a typical catalyst slurry sampling procedure, about 7–8 g of catalyst slurry was purged and then 2–3 g of catalyst slurry was collected as representative sample from the reactor at the time of sampling.

2.3 Mössbauer Spectroscopic Measurements

Mössbauer spectra were collected in a transmission mode by a standard constant acceleration spectrometer (MS-1200, Ranger Scientific). A radiation source of 30 mCi ^{57}Co in Rh matrix was used and spectra were obtained using a gas detector. The catalyst samples collected from the CSTR were in the rewax/PW3000 matrix that was a solid at room temperature. This solid matrix was mounted in plexiglass compression holders that present a thin aspect to the γ-ray beam. All samples were investigated at room temperature as well as at cryogenic temperatures, typically over a velocity range of ± 10 mm/s. For the low temperature measurements, the samples were placed inside a vibration free closed cycle cryostat (Cryo-Industries of America). The structural analysis of the samples was done by least-squares fitting of the Mössbauer spectra to a summation of hyperfine sextets. The least-square fitting

procedure was done with user defined functions within the PeakFit program. The parameters for each sextet in the fit consisted of the position, width and height of the first peak, the hyperfine magnetic field, and the quadrupole electric field. These parameters were allowed to vary freely to obtain the best fit of the experimental data. Errors in the determined percent Fe values are about ±3% for well-resolved spectra; in those that contain several iron oxide and carbide phases the uncertainty increases with the complexity of the spectrum (i.e., depending on the degree of overlapping and the weakness of the signal). However, these complex spectra are obtained during the course of change from a predominantly iron carbide or iron oxide phase and conform to a greater trend.

2.4 EXAFS and XANES Measurements

EXAFS and XANES studies were carried out at the K-edge of Fe for catalysts 1.44RbC and 5RbC, as well as reference materials, including a Fe metallic foil, Fe_2O_3, Fe_3O_4, and an iron carbide reference material. XANES spectra were also recorded at the K-edge of rubidium for catalysts 1.44RbC and 5RbC after 180 h of reaction, and for catalyst 5RbN directly after activation and after 25 h of Fischer–Tropsch reaction. In addition, spectra were recorded for two rubidium oxide reference materials, a rubidium hydroxide material, and a rubidium carbonate reference. All the XANES measurements were conducted at the National Synchrotron Light Source (NSLS) at Brookhaven National Laboratory (BNL), using beamline X18b equipped with a Si(111) channel cut monochromator. A crystal detuning procedure was employed to prevent glitches arising from harmonics. The second crystal of the channel cut monochromates is weakly linked to the crystal and slightly spring loaded. The other side is a picomotor, a very fine high pitch screw that turns by piezo, which allows for slight detuning of the crystal. The X-ray ring at the NSLS has a flux of 1×10^{10} photons per second at 100 mA and 2.5 GeV, and the energy range capability at X18b is 5.8–40 keV. The catalysts samples withdrawn from CSTR were suspended in the Fischer–Tropsch wax matrix which acted as a protective coating for the active catalysts and also prevents any air oxidation. XANES data were recorded near the iron or rubidium K-edge after cooling under He flow to liquid N_2 temperatures. To obtain a second rubidium oxide reference, RbOH was heated to 275 °C in flowing helium and held for 20 min at that condition prior to cooling to liquid nitrogen temperature.

At the Fe K-edge, for the 1.44RbC and 5RbC catalysts, an EXAFS comparison of the k^3-weighted Fourier Transform magnitude spectrum with the Fe reference spectra (i.e., Fe^0, iron carbide, Fe_2O_3, and Fe_3O_4) was carried out and a qualitative comparison is provided. All EXAFS spectra were recorded at close to the boiling temperature of nitrogen in an in situ flow cell to minimize the contribution from the dynamic Debye–Waller factor. Data reduction of the EXAFS spectra was carried out with WinXAS [15]. Standard data reduction was carried out by pre-edge background removal using two 2nd order splines and normalization by division of the height of the absorption edge. After conversion to k-space, a cubic weighted eight section spline was using to obtain the $k^3 \times \chi(k)$ data in the single scattering region after the edge jump. The Δk window used was 2– 14.75 $Å^{-1}$ prior to application of the Fourier transform in obtaining the phase uncorrected radial distribution function.

Data reduction of the XANES spectra was carried out with WinXAS. Standard data reduction was carried out by pre-edge background removal and normalization by division of the height of the absorption edge. In the case of the iron K-edge data, linear combination fitting of the experimental catalysts with select references was carried out using WinXAS over the range energy range of 7.1–7.16 keV for Fe. For rubidium, the catalysts were compared to references over the range 15.15–15.25 keV.

3 Results and Discussion

3.1 Promotion Effect of Rb on Catalytic Activity, Stability and Product Selectivity

As the basis for the comparison of effect of the composition on catalytic activity, stability, and product selectivity, Fischer–Tropsch synthesis were conducted with unpromoted, 1.44RbC and 5RbC catalyst at identical reaction conditions. The initial catalytic activity of the unpromoted catalyst was found to be almost double that of 5RbC—the promoted catalyst results in a CO conversion which is 0.56 times that of the unpromoted catalyst (Fig. 1). However, the rate of deactivation of the unpromoted catalyst was more rapid than for the promoted catalyst. It should be noted that apart from catalyst deactivation during FTS, the withdrawal of the catalyst samples during the experiment also contributed to the decrease in conversion. Since the amounts of catalyst withdrawn were roughly the same for both of the experiments, a direct comparison of deactivation rates between the two experiments appears justified. In the case of the unpromoted catalyst, CO conversion changed from 85 to 10% over a synthesis period of 300 h; with 5RbC, the change in CO conversion level was ca. 48–25% over 600 h of reaction. The decrease in CO conversion in the case of the unpromoted catalyst was 3.12% per day while in the case of promoted (5RbC), it was found to be 0.97% per day. Thus the rubidium promoted catalyst

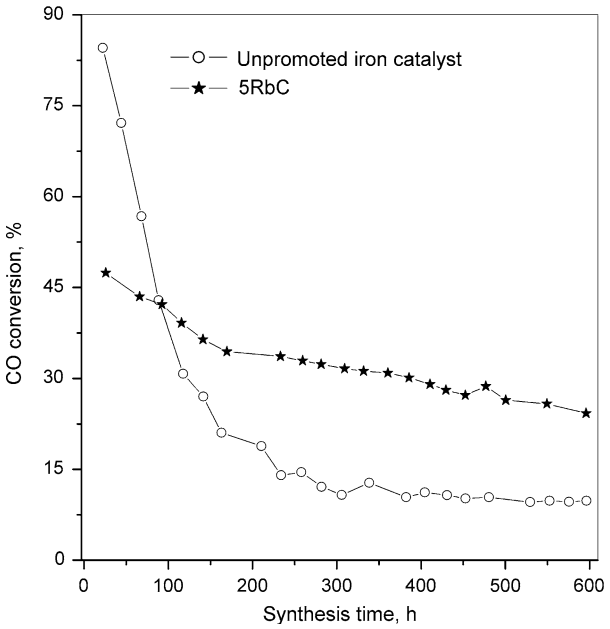

Fig. 1 Variation of CO conversion against synthesis time for unpromoted ultrafine catalyst and 5RbC. FTS effected at 270 °C, 175 psig, $H_2/CO = 0.7$, and a syngas space velocity of 3.0 sl/h/g Fe

results in a more steady conversion level. It can be mentioned that, the product selectivities of the unpromoted and promoted catalysts were not similar (as discussed later), the reaction environment (i.e., partial pressure of H_2, CO, CO_2 and H_2O) that the catalyst experience was also different. Hence, it is possible that the "intrinsic deactivation rate" of these catalysts is different than the observed deactivation rate. However, it is the "observed deactivation rate" which has significance for the purpose of commercial operation. The α-value of the unpromoted catalyst was found to be 0.85 while that of 5RbC it was 0.93 showing the promotional effect of rubidium for heavy hydrocarbon formation.

The alkene/(alkene + alkane) fraction for C_2 and C_3 hydrocarbon products from FTS for unpromoted catalyst and 5RbC are shown in Fig. 2a and b, respectively. Promotion of rubidium in 5RbC results in a C_2 alkene ratio which is more than twice the value corresponding to that of unpromoted catalyst (Fig. 2a). In the case of the C_3 hydrocarbon fraction, the alkene ratio for 5RbC was only slightly higher than that of unpromoted catalyst (Fig. 2b). A similar trend was observed for C_4 hydrocarbon fraction also. These results indicate that addition of rubidium as a promoted enhances the olefin selectivity in FTS. The 1-alkene/2-alkene fraction was found to be higher for 5RbC than the unpromoted catalyst (Fig. 3) indicating inhibition of secondary reactions of 1-alkenes by the addition of rubidium. Initial production of methane in the case of unpromoted catalyst was found to be significantly higher than rubidium promoted 5RbC catalyst (Fig. 4a). However, after about 200 h of synthesis time, the methane selectivity for both of the catalysts was found to be similar.

CO can be converted either into hydrocarbon products and water (via FTS) or into CO_2 and H_2 (via WGS reaction). A reversible WGS reaction accompanies the FTS over iron-based catalyst only at high temperature conditions. The individual rate of FTS (r_{FTS}) and WGS reaction (r_{WGS}) can be calculated from experimental results as: $r_{WGS} = r_{CO_2}$ and $r_{FTS} = r_{CO} - r_{CO_2}$ where r_{CO_2} is the rate of CO_2 formation and r_{CO} is the rate of CO conversion. Since, the WGS

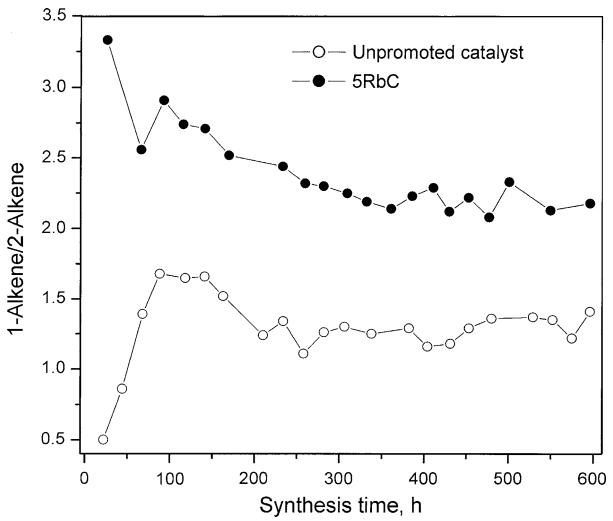

Fig. 3 Comparison of 1-alkene/2-alkene ratio for unpromoted ultrafine catalyst and 5RbC. FTS effected at 270 °C, 175 psig, $H_2/CO = 0.7$, and a syngas space velocity of 3.0 sl/h/g Fe

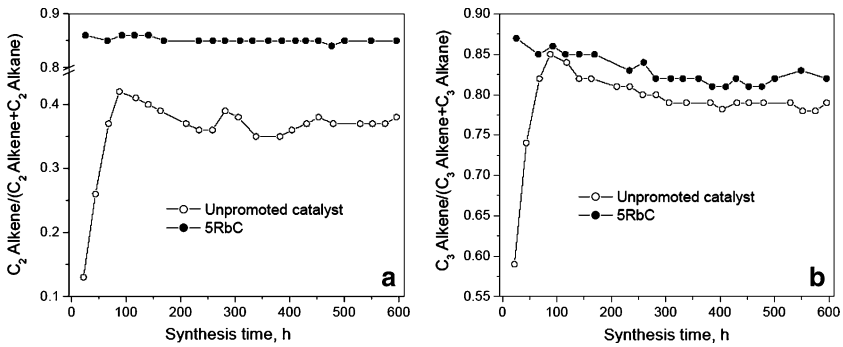

Fig. 2 Comparison of (**a**) the ratio of C_2 alkene to total C_2 hydrocarbon (i.e., alkene and alkane); and (**b**) the ratio of C_3 alkene to total C_3 hydrocarbon (i.e., alkene and alkane) produced for unpromoted ultrafine catalyst and 5RbC. FTS effected at 270 °C, 175 psig, $H_2/CO = 0.7$, and a syngas space velocity of 3.0 sl/h/g Fe

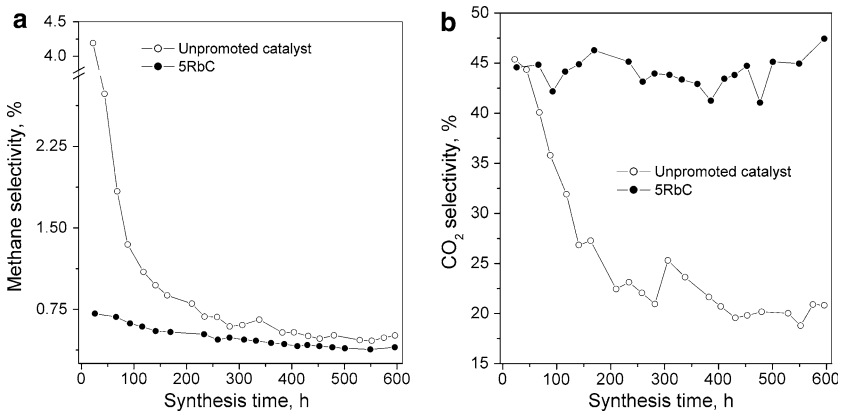

Fig. 4 Comparison of (**a**) methane selectivity; and (**b**) CO_2 selectivity for unpromoted ultrafine catalyst and 5RbC. FTS effected at 270 °C, 175 psig, $H_2/CO = 0.7$, and a syngas space velocity of 3.0 sl/h/g Fe

reaction consumes the water produced by the FTS, an inequality, $r_{FTS} \geq r_{WGS}$, is always true. CO_2 can also be formed by disproportionation of CO as: $2CO \leftrightarrow CO_2 + C$ (Boudouard reaction). At a similar conversion level, the CO_2 selectivity indicates the WGS activity of two catalysts. The CO_2 selectivity in the present study is calculated as: CO_2 selectivity, % = (ratio of moles of CO_2 produced to moles of CO converted per hour) × 100. The initial CO_2 selectivity for the unpromoted and the 5RbC catalyst were similar (Fig. 4b); however, after about 100 h of synthesis time the CO_2 selectivity for the unpromoted catalyst was significantly lower (about 25%) than the 5RbC catalyst (about 45%). A direct comparison of WGS activity between the unpromoted and 5RbC catalysts is not probably justified due to the rapid decrease in CO conversion for the unpromoted catalyst. It was reported that addition of rubidium (with a Rb/Fe atomic ratio of 1.44/100) as a promoter results in a decrease of both the FTS and WGS rate compared to unpromoted catalyst [2]. However, the difference in the corresponding rates between the unpromoted and promoted catalyst was higher at a higher space velocity. At a space velocity of 30 sl/h/g Fe, the WGS rate of the unpromoted catalyst was significantly higher than 1.44RbC, while at a space velocity of 10 sl/h/g Fe, the two rates were comparable [2]. In the present study at a space velocity of 3.0 sl/h/g Fe, it was observed that the CO_2 selectivity of 5RbC catalyst is higher than unpromoted catalyst at a similar CO conversion (about 100 h of synthesis time). The effect of Group I alkali metal promoters on the WGS activity were reported by several researchers although the mechanism by which rubidium or similar alkali metal promoters promotes WGS activity for iron catalyst is not well understood [2, 7, 9, 10].

3.2 Iron Phase Composition by Mössbauer Spectroscopy

Dynamic phase transformation of iron species in the catalyst during carbidization and FTS was monitored by Mössbauer spectroscopy. Analyzed Mössbauer spectra for unpromoted and 5RbC catalysts are shown in Fig. 5a–f. All of the Mössbauer spectra in the present study represented a complex pattern comprised of magnetite, carbide and paramagnetic components. The extent of the resulting magnetic hyperfine splitting was in the range typical of the iron carbides [16]. The characteristic shape of the individual magnetic component indicates the presence of three distinct sextets. It is known that Mössbauer spectra of ε, χ, χ' and χ'' iron carbides contain three distinct sextets, while the Mössbauer patterns of ε' and θ iron carbides appear as single sextet [17]. Reliable identification of different carbide phases was performed based on the number of constituent sextets, corresponding hyperfine magnetic fields, and their relative intensities. Compositional changes in terms of percent peak area of the different iron species as determined from curve fitting for all the samples along with corresponding sampling times are listed in Table 1 for spectra recorded at two different temperatures.

Phase transformation during activation and evolution of the active phase under FTS determine the performance of the catalyst. It is known that during the activation (using either CO, H_2 or syngas) process, iron oxide (hematite, α-Fe_2O_3) transforms quickly to magnetite (Fe_3O_4) which converts to different iron phases depending on activation environment. Activation using H_2 results in metallic iron (Fe^0) which evolves slowly into mixture of iron carbides and oxides on exposure to syngas during FTS [18]. When CO or syngas is used for activation, based on initial composition of the catalyst, different types of iron carbides have been identified [19, 20]. In general, CO activation was found to lead to a higher fraction of carbide phase and to high catalytic activity than similar syngas or H_2 activation. The fraction of iron present as the carbide following the activation was found to be dependent on catalyst composition. Zarochak and McDonald [21] studied the effect of pretreatment on the activity and the selectivity of slurry phase FTS with a potassium promoted precipitated iron catalyst and characterized the catalyst by Mössbauer

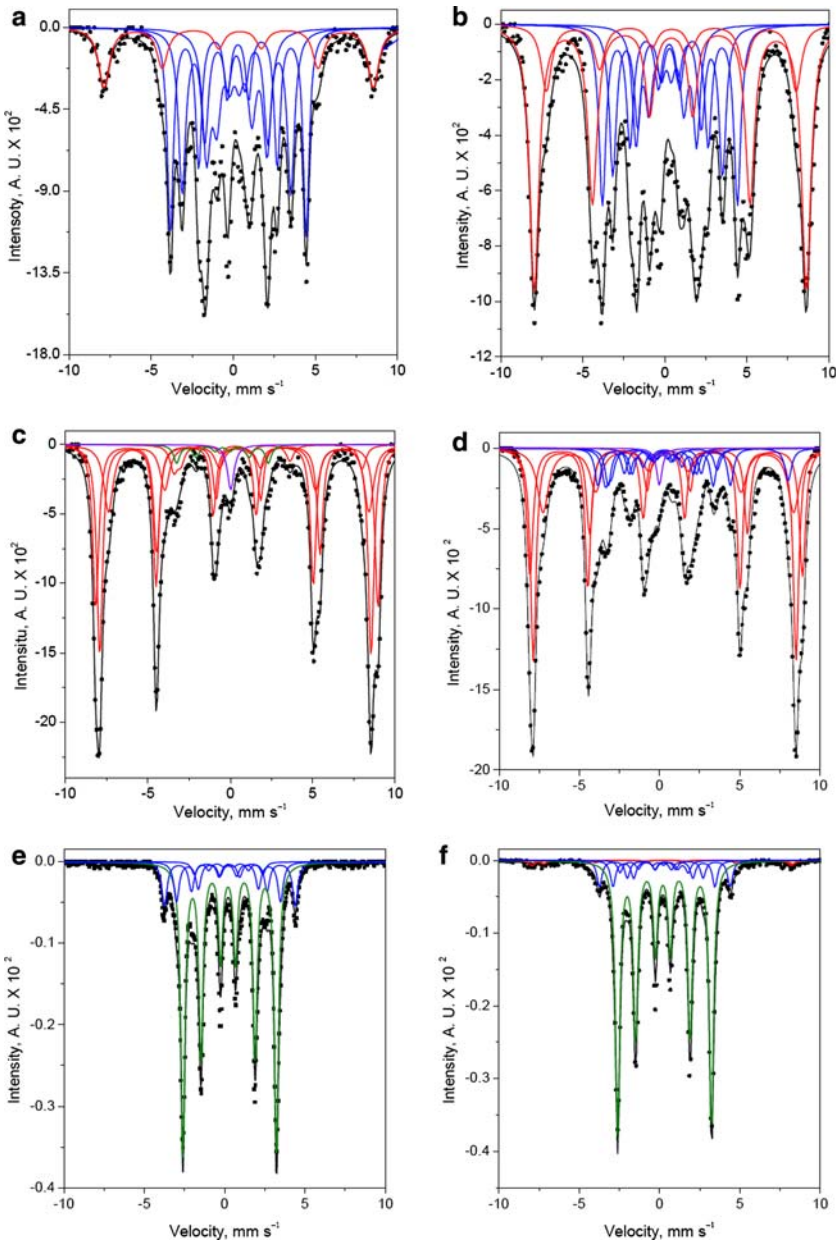

Fig. 5 Representative Mössbauer spectra of promoted and unpromoted catalyst samples collected after activation and during FTS at 270 °C, 175 psig, $H_2/CO = 0.7$, and a syngas space velocity of 3.0 sl/h/g Fe: (**a**) unpromoted catalyst sample collected after carbidization with CO for 24 h at 270 °C, 175 psig, and a space velocity of 3.0 sl/h/g Fe; (**b**) unpromoted catalyst sample collected after 28.9 h of synthesis; (**c**) unpromoted catalyst sample collected after 481.6 h of FTS; (**d**) 5RbC catalyst sample collected after carbidization with CO for 24 h at 270 °C, 175 psig, and a space velocity of 3.0 sl/h/g Fe; (**e**) 5RbC catalyst sample collected after 115.7 h of synthesis; and (**f**) 5RbC catalyst sample collected after 361.7 h of FTS. The fitted curves are shown in solid lines: black, total envelop spectra; red, oxide; blue, χ-Fe_5C_2; green, ε'-$Fe_{2.2}C$; and violet, spm phase

spectroscopy. Prior to FTS the catalyst was activated for 24 h using CO and syngas. It was found that the catalyst activated in CO was completely converted in χ-Fe_5C_2 while the catalyst activated in syngas was converted partly to ε'-$Fe_{2.2}C$ during 24 h activation, and was completely converted to ε'-$Fe_{2.2}C$ only after 503 h of FTS. The FTS activity and stability of the catalyst subjected to CO pretreatment was found to be higher than that found for the catalyst activated in syngas.

In the case of the unpromoted iron catalyst, carbidization with CO results in a transformation from hematite (Fe_2O_3) to magnetite (Fe_3O_4) and then finally to iron carbide [22, 23]. The conversion of hematite to magnetite is generally very rapid and difficult to monitor unless special attention is paid [24]. At the end of the 24 h activation period (sample S1, Table 1), the room temperature Mössbauer results revealed that for the unpromoted catalyst, about 85% of the iron phase in the catalyst was present as Hägg carbide () with the remaining iron phase present as a superparamagnetic (spm) form. Low-temperature (20 K) Mössbauer measurements, however, indicated that the spm phase was Fe_3O_4, and not the iron carbide, which can also be present in a spm phase. Thus carbidization of the unpromoted catalyst with CO at 270 °C for 24 h converted the initial hematite to a mixture of 85% and 15% Fe_3O_4 in agreement to the results reported earlier [25].

However, in the case of the rubidium promoted catalyst, the extent of carbidization with CO was found to be lower

Table 1 Summary of phase identification of iron from Mössbauer spectroscopy analysis

Sample #	Catalyst details	FTS time (h)	Fraction of Fe at 300 K (%)	Fraction of Fe at 20 K (%)
S1	Unpromoted iron oxide	0 (After 24 h carbidization)	85 in χ-Fe_5C_2 15 in spm	84 in χ-Fe_5C_2 16 in Fe_3O_4
S2	Unpromoted iron oxide	28.9	33 in Fe_3O_4 48 in χ-Fe_5C_2 19 in spm	50 in Fe_3O_4 50 in χ-Fe_5C_2
S3	Unpromoted iron oxide	481.6	93 in Fe_3O_4 7 in γ-Fe_2C	93 in Fe_3O_4 5 in ε'-$Fe_{2.2}C$ 2 in spm
S4	5RbC	0 (After 24 h carbidization)	73 in Fe_3O_4 15 in χ-Fe_5C_2 12 in spm	82 in Fe_3O_4 17 in χ-Fe_5C_2 1 in spm
S5	5RbC	115.7	27 in χ-Fe_5C_2 66 in ε'-$Fe_{2.2}C$ 7 in spm	29 in χ-Fe_5C_2 71 in ε'-$Fe_{2.2}C$
S6	5RbC	361.7	13 in χ-Fe_5C_2 82 in ε'-$Fe_{2.2}C$ 5 in spm	3 in Fe_3O_4 21 in χ-Fe_5C_2 76 in ε'-$Fe_{2.2}C$
S7	1.44RbC	180	–	53 in ε'-$Fe_{2.2}C$ 33 in χ-Fe_5C_2 9 in Fe_3O_4 5 in spm

than for the unpromoted catalyst. At the end of the carbidization period, ca. 17% of was found to be present in the catalyst (sample S4, Table 1). The carbidization of rubidium promoted catalyst continued with FTS (i.e., in situ reduction by syngas). After continuous FTS over a long period, all the iron species in the 5RbC catalyst was nearly found to be present as carbides (sample S5 and S6). Two phases of carbide were identified in 5RbC, namely and Activation of an iron based catalyst with syngas is known to predominantly result in ε'-$Fe_{2.2}C$ as the main carbidic phase [22, 26]. Since the catalyst after 24 h carbidization with CO did not contain the ε'-$Fe_{2.2}C$ phase, this hexagonal carbide phase was definitely generated by in situ carbidization with syngas during FTS. The fraction of was found to decrease while the fraction of was found to increase with increasing synthesis time (i.e., syngas exposure time). The nature of the iron phase composition of 1.44RbC catalyst followed a trend similar to that of 5RbC. However, the fraction of the carbide phases (and ε'-$Fe_{2.2}C$) present after 180 h of FTS was found to be lower (sample S7) than the corresponding amount found in 5RbC (sample S5) after ca. 115 h of synthesis. The above results indicate that the extent of in situ carbidization (or the resistance to re-oxidation) may be strongly dependent on the Rb/Fe atomic ratio and the presence of some high fraction of iron carbide is probably necessary for a catalyst to exhibit high conversion in FTS.

3.3 EXAFS and XANES Measurements

Normalized absorptivity versus energy plots in the near edge region, along with the corresponding derivative spectra for the iron K-edge data, are represented in Figs. 6 and 7, respectively. Qualitative examination of the normalized XANES spectra reveals that the spectrum corresponding to the activated 5RbC and 1.44RbC catalyst matches most closely to that of the iron carbide reference material. A better qualitative comparison can be made by considering the derivative spectra obtained from the normalized absorptivity XANES spectra (Fig. 7). This is because the derivative spectra can pick up key inflections in the onset of absorption that are difficult to detect by analysis of the normalized absorptivity spectra. It is qualitatively evident that the activated 5RbC catalyst matches most closely with that of the iron carbide reference spectra and the overall spectral pattern of 1.44RbC also follow the shape of iron carbide reference spectra. Not only do the peak positions match very closely (large peak at about 7.123 keV and two shoulders at about 7.118 and 7.128 keV), but their intensities are also relatively similar, with excellent agreement observed especially in the shape, intensity, and position of the onset peak (7.112 keV). The small peak (shoulder) at 7.118 keV for the iron carbide reference, 5RbC and 1.44RbC samples suggest a mild degree of oxidation, most likely confined to a passivation

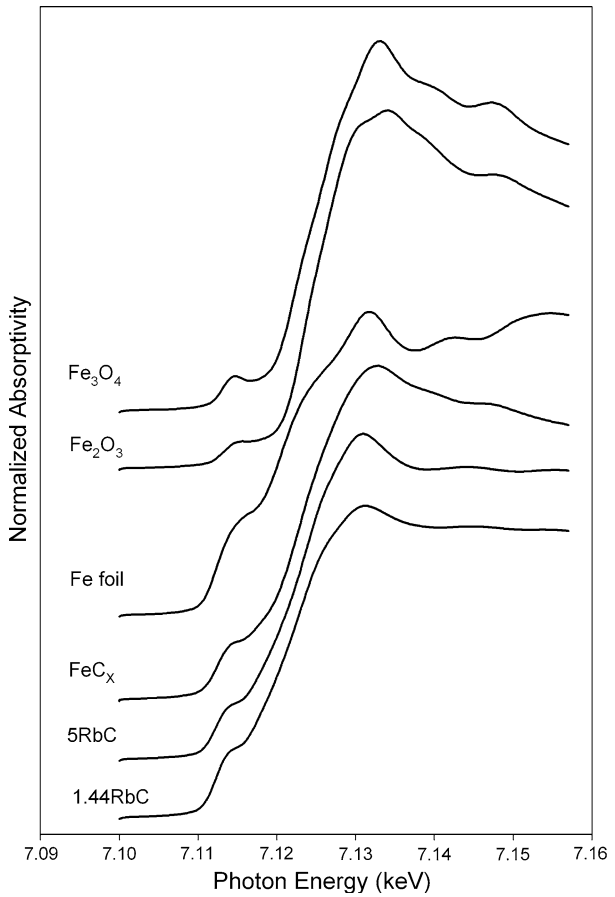

Fig. 6 Normalized XANES spectra at Fe K-edge of references and active 5RbC and 1.44RbC catalyst

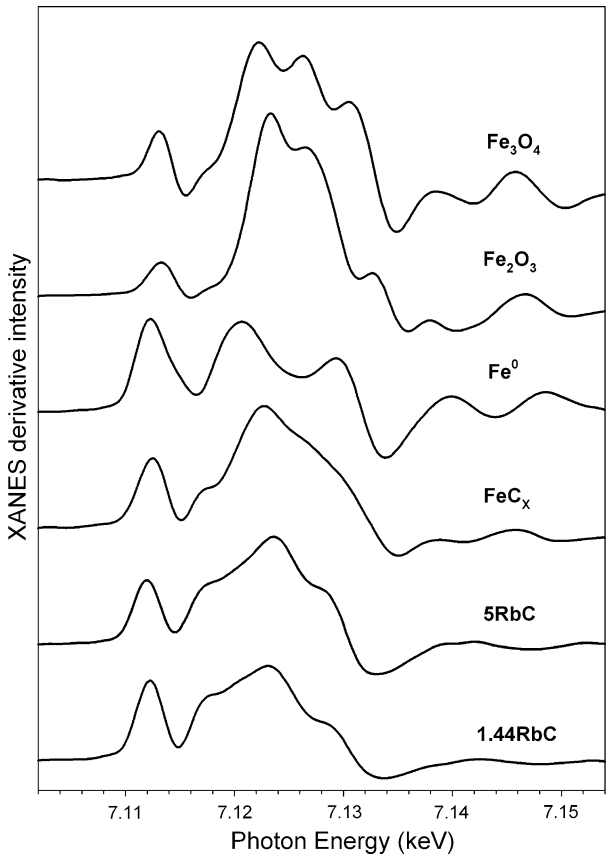

Fig. 7 XANES derivative spectra at Fe K-edge of references and used 5RbC and 1.44RbC catalysts

layer in the surface shell, as this peak matched very closely a peak observed in the iron oxide reference materials. XANES fittings of the spectra for the active working catalysts with a linear combination of the reference spectra [27] suggest that iron carbides are a major constituent which also supports the results from Mössbauer spectroscopy measurement.

Fourier transformed magnitude spectra for the Fe K-edge data are presented in Fig. 8. The Fe–Fe coordination peaks for 1.44RbC and 5RbC samples are in good agreement with those observed for the iron carbide reference sample at approximately 1.6, 2.1 and 2.5 Å (shoulder peak for 1.44RbC and 5RbC). Furthermore, there are low R peaks (e.g., ~1.5 Å) that exhibit good agreement with the iron carbide reference, and may correspond to Fe–C coordination. However, it is not possible to rule out Fe–O coordination from the contribution of Fe-oxide in the samples. The above results indicate that a major fraction of working catalyst is composed of iron carbides.

Figure 9 presents the XANES spectra taken at the Rb K-edge of 5RbC (after 180 h of FTS), 5RbN (after activation and 25 h of FTS), 1.44RbC (after 180 h of FTS) and several rubidium reference samples. This allows a direct comparison of the catalysts 5RbN, 5RbC, 1.44RbC, and various reference materials, including RbOH, Rb_2CO_3, and two different Rb_2O references (one that was purchased, and the one prepared from the in-situ decomposition of RbOH at 275 °C in helium flow). The reason that the RbOH decomposition was carried out was due to reported problems with the differentiation of Rb compounds as reported in earlier studies [12]. Shape of the spectra and peak position for the four catalyst samples match closely with the spectra of rubidium carbonate reference sample. The pattern of normalized XANES spectra of activated 5RbN and working 5RbN samples (sample after 25 h of FTS) follow significant similarity with rubidium carbonate reference spectra indicating that rubidium may exist as rubidium carbonate in these two catalysts. Since the decomposition temperature of rubidium nitrate is 219 °C and carbidization/FTS was performed at 270 °C, the rubidium nitrate precursor might transform into rubidium carbonate by the presence of CO_2 during carbidization/FTS. An overlay of all catalyst samples with the Rb_2CO_3 reference sample (shown at the top of Fig. 9) indicate very strongly that the active state of the rubidium promoter was an oxidized state of +1, and that the chemical species

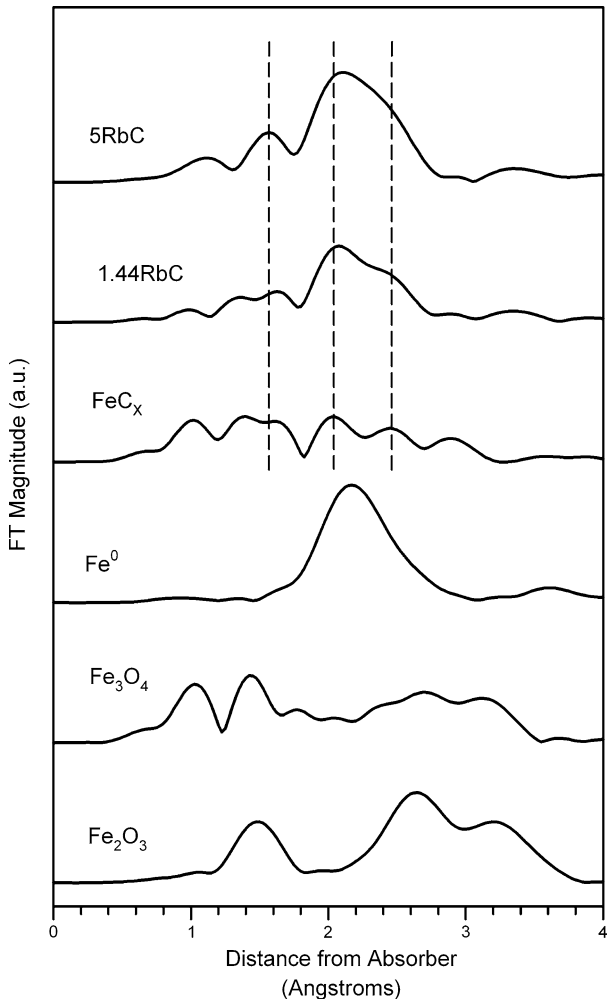

Fig. 8 EXAFS Fourier transformed magnitude spectra at Fe K-edge of references and used 5RbC and 1.44RbC catalysts

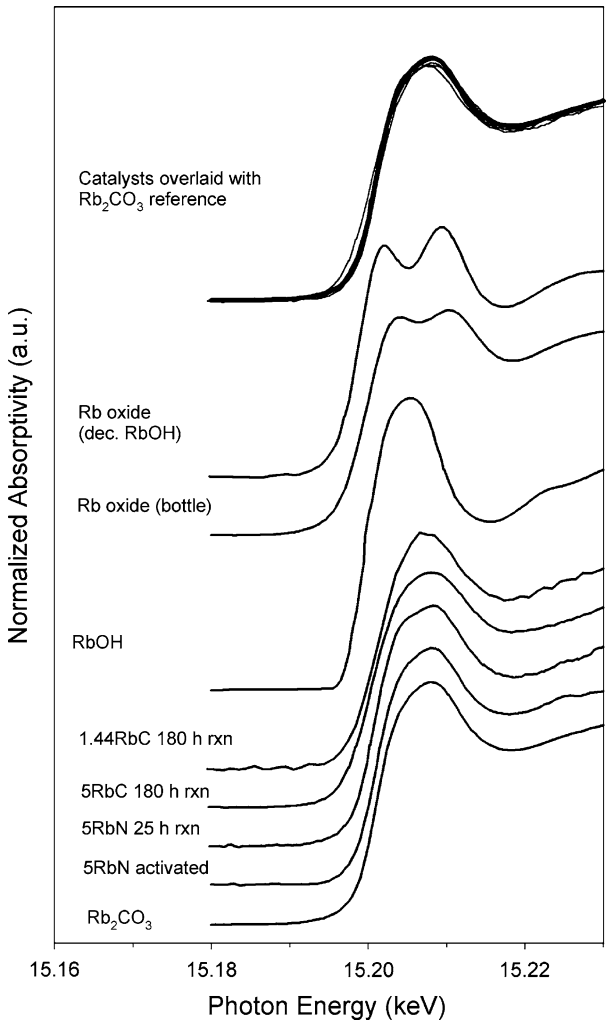

Fig. 9 Rb K-edge XANES spectra of, moving upward, Rb_2CO_3 reference, the activated 5RbN catalyst, the activated 5RbN catalyst after 25 h on stream, the activated 5RbC catalyst after 180 h on stream, the 1.44RbC catalyst after 180 h on stream, an Rb_2O sample purchased, an Rb_2O sample prepared from the decomposition of RbOH in helium at 275 °C, and an overlay of all the catalyst samples with the Rb_2CO_3 reference

present in the working catalyst was likely rubidium carbonate.

It is not clear at this time if the rubidium carbonate was the actual promoter for FT selectivity, or if the rubidium carbonate was a spectator and that there were a different surface species in close contact with iron carbides that was responsible for promoting effect, as has been suggested in the case of potassium [5]. However, it is notable that decreasing the rubidium content from 5.0/100 to 1.44/100 Rb/Fe atomic ratio did not lead to a significant change in the XANES spectra white line shape or intensity to signify that a different chemical state of rubidium was present.

4 Conclusions

Promoting iron based catalyst with rubidium results in a steady conversion rate in FTS relative to the unpromoted catalyst, which despite having a higher initial conversion, deactivated quickly. Rubidium promoted catalyst have a higher alkene and 1-alkene ratio, higher CO_2 selectivity, and lower methane selectivity compared to unpromoted catalyst. Mössbauer spectroscopy measurements of unpromoted and rubidium promoted iron catalysts indicate that the carbide content of the catalyst closely follows the catalytic activity. In situ recarbidization was favored by the presence of Rb in the catalyst and ε'-$Fe_{2.2}C$ became the predominant carbide phase. Fe K-edge XANES and EXAFS spectra for the working catalyst also confirmed the presence of iron carbides as a major constituent of the catalyst under FTS conditions. XANES spectra recorded at the Rb K-edge of the active catalyst samples suggested that Rb was in an oxidized form and also that the chemical

compound most prevalent in the working FTS catalyst samples closely resembled that of rubidium carbonate.

Acknowledgments This work is supported by US DOE contract number DE-FC26-03NT41965 and the Commonwealth of Kentucky. The EXAFS/XANES experiments are carried out at the National Synchrotron Light Source, Brookhaven National Laboratory, which is supported by the US DOE, Divisions of Materials Science and Chemical Sciences. Special thanks to Dr. Syed Khalid (Beamline X18b, NSLS, Brookhaven) and Dr. Patricia M. Patterson, Center for Applied Energy Research, U of Kentucky, Lexington, KY for help with XAFS studies.

References

1. Ronald D, Bell AT (1986) J Catal 97:121
2. Ngantsoue-Hoc W, Zhang Y, O'Brien RJ, Luo M, Davis BH (2002) Appl Catal 236:77
3. Li S, Li A, Krishnamoorthy S, Iglesia E (2001) Catal Lett 77:197
4. Li S, Ding W, Meitzner GD, Iglesia E (2002) J Phys Chem B 106:85
5. Li S, Krishnamoorthy S, Li A, Meitzner GD, Iglesia E (2002) J Catal 206:202
6. Luo M, O'Brien RJ, Bao S, Davis BH (2003) Appl Catal A Gen 239:111
7. Arakawa H, Bell AT (1983) Ind Eng Chem Res Process Des Dev 22:97
8. Raje AP, O'Brien RJ, Davis BH (1998) J Catal 180:36
9. Bukur DB, Mukesh DS, Patal A (1990) Ind Eng Chem Res 29:194
10. Dictor RA, Bell AT (1986) J Catal 97:121
11. Miller DG, Moskovits M (1988) J Phys Chem 92:6081
12. Doskocil EJ, Bordawekar SV, Davis RJ (1997) J Catal 169:327
13. Tsuchiya S, Takase S, Imamura H (1984) Chem Lett 5:661
14. Tanabe K, Misono M, Ono Y, Hattori H (1989) New solid acids and bases. Kodansha, Tokyo
15. Ressler T (1997) WinXAS97 version 1.0
16. Niemantsverdriet JW, van der Krann AM, van Dijk WL, van der Baan HS (1980) J Phys Chem 84:3363
17. Butt JB (1990) Catal Lett 7:61
18. Dry ME (1981) In: Anderson JR, Boudart M (eds) Catalysis—science and technology. Springer-Verlag, New York, p 59
19. Huang C-S, Ganguly B, Huffman GP, Huggins FE, Davis BH (1993) Fuel Sci Technol Int 11(9):1289
20. Hofer LJE (1956) In: Emmett PH (ed) Catalysis, vol IV. Reinhold Publishing, New York, pp 373–442
21. Zarochak MF, McDonald MA (1986) Slurry-phase Fischer–Tropsch synthesis, CONF-86/288-1, Proceedings of indirect liquefaction contractor's conference, Monroeville, PA, USA, December 2–4, 1986
22. Davis BH (1999) Technology development for iron Fischer–Tropsch catalysis, US DOE Final Technical Report, Contract # DE-AC22-94PC94055-13
23. Sarkar A, Seth D, dozier AK, Neathery JK, Hamdeh HH, Davis BH (accepted, in press) Catal Lett
24. Sarkar A, Dozier AK, Graham UM, Thomas G, O'Brien RJ, Davis BH (2007) Appl Catal A Gen 326:55
25. Rao KRPM, Huggins FE, Huffman GP, Gormley RJ, O'Brien RJ, Davis BH (1996) Energy Fuels 10:546
26. Rao KRPM, Huggins FE, Huffman GP, O'Brien RJ, Gormley RJ, Davis BH (1995) Prepr Pap ACS Div Fuel Chem 40(1):153
27. Li S, Meitzner GD, Iglesia E (2001) J Phys Chem B 105:5743